Journal of Alloys and Compounds 495 (2010) 334–337

Contents lists available at ScienceDirect

Journal of Alloys and Compounds

journal homepage: www.elsevier.com/locate/jallcom

Crystallisation behaviour and glass-forming ability in Al–La–Ni system

P. Gargarella [a,*], C.S. Kiminami [b], M.F. de Oliveira [c], C. Bolfarini [b], W.J. Botta [b]

[a] Programa de Pós-Graduação em Engenharia e Ciência dos Materiais, Departamento de Engenharia de Materiais, Universidade Federal de São Carlos, Rod. Washington Luis Km 235, 13565-905, São Carlos, SP, Brazil
[b] Departamento de Engenharia de Materiais, Universidade Federal de São Carlos, Rod. Washington Luis Km 235, 13565-905, São Carlos, Brazil
[c] Departamento de Engenharia de Materiais, Aeronáutica e Automobilística, Universidade de São Paulo, Av. Trabalhador Sancarlense, 400, 12560-970, São Carlos, São Paulo, Brazil

ARTICLE INFO

Article history:
Received 19 August 2008
Received in revised form 29 October 2009
Accepted 2 November 2009
Available online 10 November 2009

Keywords:
Al alloys
Metallic glasses
Rapid-solidification
Phase transitions

ABSTRACT

The crystallisation behaviour for alloys in the Al-rich corner in the Al–La–Ni system is reported in this paper. Alloys were selected based on the topological instability criterion (λ criterion) calculated from the alloy composition and metallic radii of the alloying elements and aluminum. Amorphous ribbons were produced by melt-spinning and the crystallisation reactions were analysed by X-ray diffraction and calorimetry. The results showed that increasing the values of λ from 0.072 to 0.16 resulted in the following changes in the crystallisation behaviour, as predicted by the λ criterion: (a) nanocrystallisation of α-Al for the alloy composition corresponding to λ = 0.072 and (b) detection of the glass transition temperature, T_g, for the alloys with composition close to λ ≈ 0.1 line. For compositions corresponding to both ends of the λ ≈ 0.1 line (near the binaries lines) T_g could be detected only in the "intermediary" central region, and the alloy we produced in this region was considered the best glass former for the Al-rich corner. Also, except for the alloys with the highest Ni content, crystallisation proceeded by two distinct exothermic peaks which are typical of nanocrystallisation transformation. These behaviours are discussed in terms of compositional (λ parameter) and topological aspects to account for cluster formation in the amorphous phase.

1. Introduction

The topological instability concept was first proposed [1] to predict the composition limits for amorphization of binary Al-based alloys. Such limit was associated with the minimum solute concentration necessary to de-stabilize, due to elastic tension, a crystalline solid solution with the same composition of the liquid. This criterion was extended to predict the crystallisation behaviour of multicomponent Al-rich amorphous alloys [2,3]. In this proposition the λ parameter is calculated for an $Al_{cAl}B_{cB}C_{cC}D_{cD}\ldots Z_{cZ}$ alloy (where B to Z are different TM or RE solute elements and c_i are the corresponding compositions) as the ratio of solute atoms to Al radius defined by Eq. (1):

$$\lambda = \sum_{i=B}^{Z} c_i \cdot \left| \frac{r_i^3}{r_{Al}^3} - 1 \right| \quad (1)$$

The thermal behaviour for many multicomponent Al-based alloys [4–9] could be related with the λ parameter since is able to indicate alloy compositions which, upon continuous heating, exhibit a supercooled liquid region (here defined as glassy alloys, with λ > 0.1), nanocrystalline behaviour (defined as nanocrystalline alloys, with λ < 0.1) or an intermediate behaviour, where nanocrystallisation is preceded by a supercooled liquid region (defined as nano-glassy alloys, with λ ≈ 0.1).

Increase of the λ values results in a clear transition from nanocrystallisation to glassy behaviour, usually with some degree of stabilization of the supercooled liquid, indicated by an increase in the crystallisation temperature. However, contrary to the expected behaviour, the best glass former composition in the Al-based systems is found to be a nano-glassy composition with λ ≈ 0.1. In the case of easy-glass former compositions of other systems, experimental evidences suggest that the best glass former compositions are related to the glassy behaviour during crystallisation [10–12].

In the present work the correlation between the λ parameter and the crystallisation behaviours in Al-rich alloys of the Al–Ni–La system is studied by comparing the glass-forming abilities for alloys with compositions corresponding to λ values close to 0.1.

2. Experimental procedure

Different alloys in the Al-rich corner of the Al–Ni–La system with compositions around λ ≈ 0.1 line were prepared, as indicated in Fig. 1. Bulk ingots of each alloy compositions were produced using an arc-melting furnace, where a mixture of high purity elements was repeatedly arc-melted in a water-cooled copper crucible in

* Corresponding author. Tel.: +55 16 3351 8549; fax: +55 16 3361 5404.
E-mail address: piterg@gmail.com.br (P. Gargarella).

0925-8388/$ – see front matter.
doi:10.1016/j.jallcom.2009.11.021

Alloy	Composition	λ
1	$Al_{80}La_{10}Ni_{10}$	0.16
2	$Al_{77}La_3Ni_{20}$	0.106
3	$Al_{80}La_5Ni_{15}$	0.114
4	$Al_{85}La_5Ni_{10}$	0.097
5	$Al_{89}La_7Ni_4$	0.102
6	$Al_{87}La_3Ni_{10}$	0.072

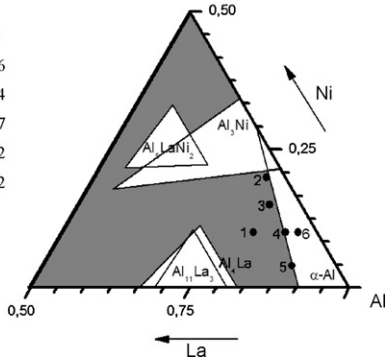

Fig. 1. Alloy compositions and position in the compositional triangle of Al–Ni–La system for Al-rich alloys. The crossing line is the $\lambda \approx 0.1$ line. The white regions correspond to $\lambda < 0.1$ and the grey region corresponds to $\lambda > 0.1$. The triangle line thus correspond to $\lambda = 0.1$ for each crystalline phase known in this system (indicated inside each triangle).

an argon atmosphere to ensure complete melting and compositional homogeneity. Then, amorphous ribbons were produced using a single-roller melt-spinning wheel at a tangential wheel speed of 42 m/s in an argon atmosphere. The approximate width and thickness of the melt-spun ribbons were 3 mm and 35 μm, respectively.

The ribbons were characterized structurally by standard X-ray diffraction (XRD) in the reflection mode using Cu-K_α radiation. The phase transformation temperatures and heat evolution during the transformations were studied by differential scanning calorimetry (DSC) at a heating rate of 20 K/min, except for $Al_{87}La_3Ni_{10}$ alloy for which it was used 30 K/min.

3. Results and discussion

The alloys 2, 3, 4 and 5 were designed to be very near the $\lambda \approx 0.1$ line and the alloys 6 and 7 had composition corresponding to $\lambda < 0.1$ and >0.1 respectively as shown in Fig. 1. The DRX results showed that with the exception of alloys 2 and 3, all the other rapidly quenched ribbons were fully amorphous.

Fig. 2 shows the XRD patterns of the alloys with compositions outside the $\lambda \approx 0.1$ line; i.e., alloys 1 and 6 (and included for comparison alloy 4 with $\lambda = 0.097$), with the expected broad peaks confirming the glassy state. Fig. 3 shows the corresponding DSC curves for the same group of alloys. Increasing the values of λ from 0.072 to 0.16 resulted in a change in the crystallisation behaviour, as predicted by the λ criterion. Nanocrystallisation of α-Al was observed only for $\lambda = 0.072$ and T_g was detected for the alloys approaching $\lambda \approx 0.1$ line, disappearing again for $\lambda > 0.1$.

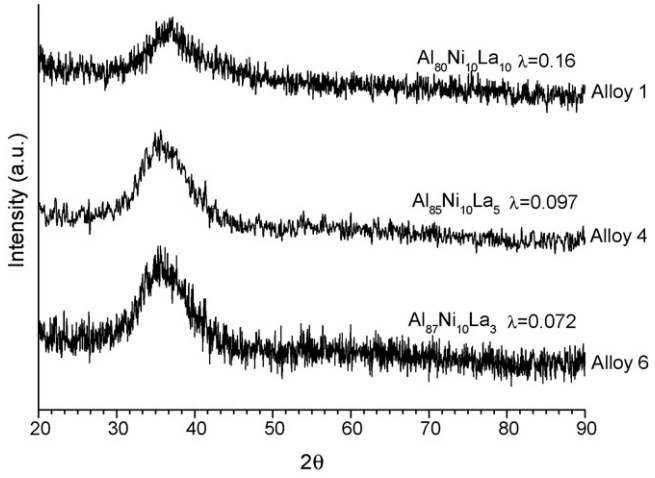

Fig. 2. XRD patterns for the melt-spun alloys with compositions outside the $\lambda \approx 0.1$ line (alloys 1 and 6) included for comparison alloy 4, as indicated in the figure.

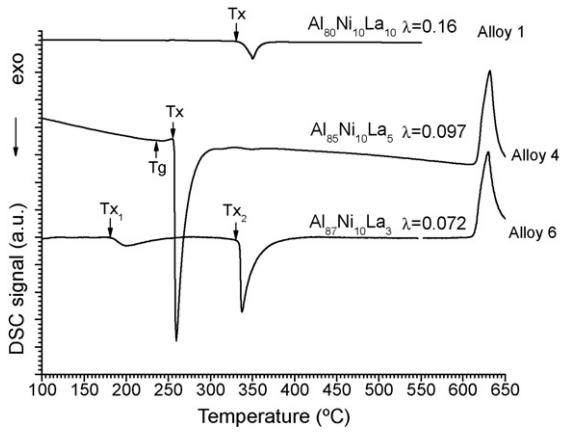

Fig. 3. DSC curves for the melt-spun alloys with compositions outside the $\lambda \approx 0.1$ line, as indicated in the figure.

These results are in complete agreement with the λ parameter in describing the crystallisation behaviour of Al-based alloys mainly for compositions in the central region of the Al-rich corner in Al–TM–RE systems.

Fig. 4 shows the XRD patterns for the as-quenched alloys prepared with compositions around the $\lambda \approx 0.1$ line, which is alloys 2, 3, 4 and 5. The alloys are ordered in increasing Ni content, with compositions varying from near the Al–La binary line to near the Al–Ni binary line. Fig. 5 shows the corresponding DSC curves, indicating the transition temperatures, T_g and T_X. In the alloys with compositions at both ends of the $\lambda \approx 0.1$ line (2, 3 and 5), no T_g was detectable, but T_g was clearly detected in the "intermediary" alloy 4. Also, except for the alloys with the highest Ni content, crystallisation proceeded by two distinct exothermic peaks which are typical of nanocrystallisation of α-Al, with suppression of T_g (alloy 5), as was seen by Botta et al. [3] for $Al_{89}Ni_{2.4}Ce_{8.6}$ alloy.

The results obtained from the thermoanalysis for alloys around the $\lambda \approx 0.1$ line are summarised in Table 1. The alloy 4, $Al_{85}Ni_{10}La_5$ was considered the best glass former in this series of alloys with ΔT_X equal to 19 °C.

The differences observed in the thermal behaviour along the $\lambda = 0.1$ line cannot be explained only by the compositional aspect related with λ parameter. Cluster configurations in the supercooled liquid must also be taken into account to justify such differences. Considering that a strong tendency to form a chemical short-range

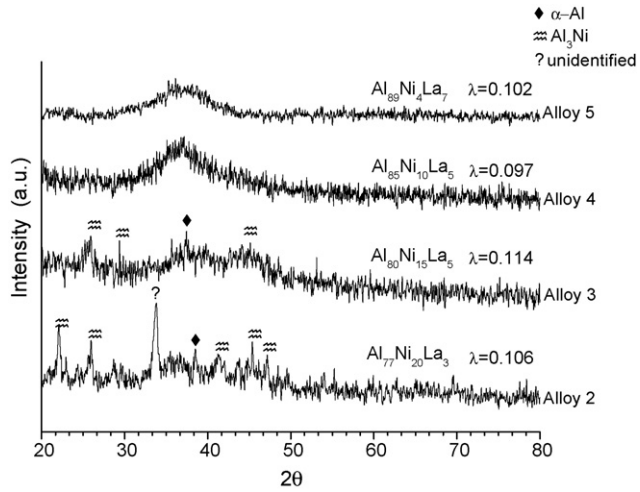

Fig. 4. XRD patterns for the alloys prepared with compositions around the $\lambda \approx 0.1$ line.

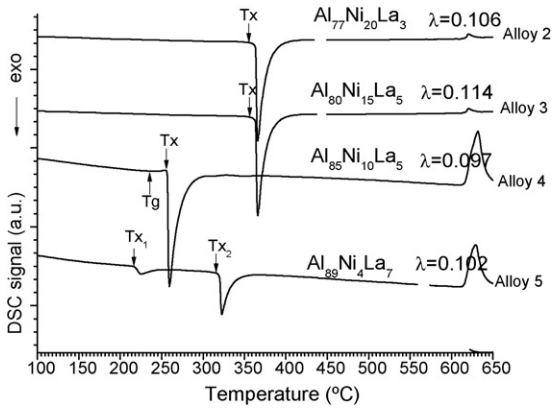

Fig. 5. DSC curves for the alloys prepared with compositions around the $\lambda \approx 0.1$ line.

order (CSRO) in the liquid state is maintained in the amorphous solid, the cluster structures must be topologically incompatible with any equilibrium crystalline structure and their stability are related with high thermal stability against crystallisation, i.e., glass formation.

For Al–TM–RE alloys, at least two distinct structural units combine in the final structure of the liquid, and their quantities and distribution can have a great influence in the thermal behaviour, as it has been reported for $Al_{85}Ni_{10}Ce_5$ and $Al_{87}Ni_{10}Ce_3$ [13,14], $Al_{90}Fe_xCe_{10-x}$ ($x = 3, 5, 7$) [15,16–18], $Al_{87}Y_8Ni_5$ and $Al_{90}Y_{10}$ [19], $Al_{100-2x}Co_xCe_x$ ($x = 8, 9, 10$) and $Al_{80}Fe_{10}Ce_{10}$ [20] alloys. In all these cases, involving Al–TM–RE systems, the existence of two distinct basic structural cluster units, RE/Al and TM/Al have been demonstrated.

In the case of TM/Al clusters a covalent nature of the chemical bonds was suggested by the observation that the atomic radii of the transition metals were reduced while the atomic radius of the Al atoms was expanded. Also, the coordination number and interatomic distances of clusters formed by TM (Fe, Ni or Co) and Al were found to be independent of the particular TM element, thus suggesting chemical similarities between Fe, Ni and Co (all of them with highly negative ΔH_{mix} with Al).

Measurements of the coordination number and interatomic distances also for RE/Al cluster, indicated an insignificant size reduction for the atoms, suggesting predominance of the metallic nature of the bonds, but a lower thermal stability against crystallisation compared with TM–Al clusters was observed. In $Al_{90}Fe_5Ce_5$ alloys [21], Fe/Al clusters were detected after the beginning of crystallisation; in $Al_{85}Ni_{10}Ce_5$ and $Al_{87}Ni_{10}Ce_3$ alloys, Ni/Al clusters were detected after the first crystallisation stage and these clusters did not change with nanocrystallisation. These observations suggest that RE/Al clusters may be predominantly associated with nanocrystallisation, justifying the slow kinetics and solute-enriched zone observed in such transformations.

We can then associate the detection of T_g only in the intermediate region of the $\lambda = 0.1$ line with the different types of cluster configurations. If there are a sufficient number of clusters associated with T_g, atomic diffusion is massive and macroscopically

Table 1
Alloy compositions, λ values and corresponding transition temperatures.

	Compositions	λ	T_g (°C)	T_X (°C)	ΔT_X (°C)
1	$Al_{80}La_{10}Ni_{10}$	0.16	–	330	–
2	$Al_{77}La_3Ni_{20}$	0.106	–	355	–
3	$Al_{80}La_5Ni_{15}$	0.114	–	356	–
4	$Al_{85}La_5Ni_{10}$	0.097	255	236	19
5	$Al_{89}La_7Ni_4$	0.102	–	315	–
6	$Al_{87}La_3Ni_{10}$	0.072	–	330	–

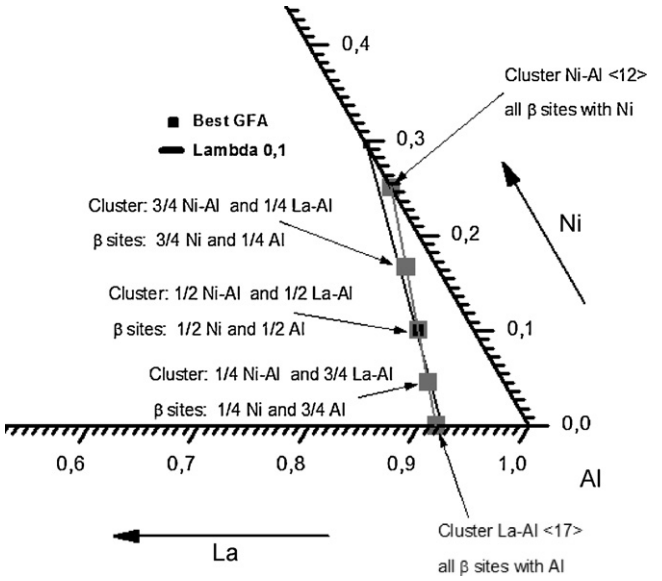

Fig. 6. Possible types of clusters mixing along the $\lambda \approx 0.1$ line and the corresponding compositions. The alloy with best GFA is indicated.

perceptible, showing a major reduction in viscosity, and T_g is detected by conventional calorimetry. The metallic nature of the bonds in RE/Al clusters and, hence, greater facilities to alter the coordination number suggest that these clusters are predominantly associated with T_g.

The nanocrystallisation behaviour observed in $\lambda < 0.1$ compositions can also be discussed based on cluster types and configurations. Depending on the cluster types and configurations, it is possible to calculate the number of Al atoms that are consumed in the formation of the clusters and possibly the number of Al atoms that are "free" in any specific composition [22]. Such free Al atoms can form a third type of cluster, Al/Al, which is topologically compatible with the crystalline structure of α-Al and can therefore justify the presence of quenched-in nuclei. If more clusters share the shell Al atoms, like in a dense-packing configuration, more "free" Al atoms will be available for primary nanocrystallisation.

The dense cluster-packing model [23] can be used to analyse the possible cluster configurations in our system, we can assume the formation of fcc cluster arrangements with the presence of interstitial atoms resulting in a highly dense packed configuration. For the Al–Ni–La system the central coordinating α atom can be either La or Ni, the β octahedral interstices can be only filled with the smallest atoms, either Al or Ni, and Ω the solvent or shell atom is Al. The possible clusters and coordination number, Nα, are La–Al with Nα = 17 and Ni–Al with Nα = 12. In the fcc arrangement, each cluster shares the solvent atoms with 12 neighbors and the number of solvent atoms per cluster can be given by $\Omega = N\alpha/(1 + 12/N\alpha)$. Thus, each La–Al cluster will have 9.96 Al atoms for each La atom and each Ni–Al cluster will have 6 Al atoms for each Ni atom.

In the Al–Ni binary compositions, considering the α sites occupied by Ni–Al clusters and the β sites occupied by Ni atoms, each cell will have a total of 8 Ni atoms (4 in the α sites and 4 in the β sites) and 24 Al atoms (6 in each of the α sites), resulting in the composition $Al_{75}Ni_{25}$. In the binary Al–La, considering the α sites occupied by La–Al clusters and the β sites occupied by Al atoms, each cell will have a total of 4 La atoms (4 in the α sites) and 43.84 Al atoms (9.96 in each of the α sites and 4 in the β sites), resulting in the composition $Al_{91.64}La_{8.36}$.

We now apply the same reasoning for ternary alloys along the $\lambda \approx 0.1$ line; in this case we must consider the mixing of the

two types of clusters and interstitial atoms. Fig. 6 indicates possible types of clusters mixing in the Al–Ni–La composition triangle, which result in $\lambda \approx 0.1$ compositions.

Clusters of the alloy compositions corresponding to $\lambda \approx 0.1$ must be arranged in such a way as to occupy all β sites by Ni and Al, in the same proportion as the proportion of Al–Ni and Al–La clusters, as indicated in Fig. 6. The experimental best glass former composition, $Al_{85}Ni_{10}La_5$, has the same number of La–Al and Ni–Al clusters suggesting that an equilibrium between these two types of cluster produce the densest cluster-packing structure, resulting in the best glass former alloy for compositions along $\lambda \approx 0.1$ line.

4. Conclusions

The correlation between the λ parameter and the crystallisation behaviours in Al-rich alloys of the Al–Ni–La system had been justified by compositional and topological approach.

The best glass former composition, $Al_{85}Ni_{10}La_5$, corresponds to $\lambda \approx 0.1$ and can be justified by the most efficient packing of the different types of clusters obtained in the centre of $\lambda \approx 0.1$ line.

Different proportions of La–Al and Ni–Al clusters and the presence and quantity "free" Al atoms in the interstitial positions among the clusters justify the different thermal behaviours along the $\lambda \approx 0.1$ line.

Acknowledgments

This work was supported by FAPESP, CAPES and CNPq.

References

[1] T. Egami, Y. Waseda, J. Non-Cryst. Solids 64 (1984) 113.
[2] R.D. Sá Lisboa, C. Bolfarini, W.J. Botta F., C.S. Kiminami, Appl. Phys. Lett. 86 (2005) 211904.
[3] W.J. Botta, C. Triveño Rios, R.D. Sá Lisboa, A.R. de Andrade, M.F. de Oliveira, C. Bolfarini, C.S. Kiminami, J. Alloys Compd. 483 (2009) 89–93.
[4] D.V. Louzguine, A. Inoue, J. Light Met. 1 (2001) 105.
[5] F.Q. Guo, S.J. Poon, G. Shiflet, Mater. Sci. Forum 331–337 (2000) 31.
[6] D.V. Louzguine, S. Sobu, A. Inoue, Appl. Phys. Lett. 85 (2004) 3758.
[7] K.L. Sahoo, M. Wollgarten, J. Haug, J. Banhart, Acta Mater. 53 (2005) 3861.
[8] D.V. Louzguine-Luzgin, A. Inoue, J. Alloys Compd. 399 (2005) 78.
[9] D.V. Louzguine-Luzgin, A. Inoue, W.J. Botta, Appl. Phys. Lett. 88 (2006) 011911.
[10] C.S. Kiminami, R.D. Sá Lisboa, M.F. de Oliveira, C. Bolfarini, W.J. Botta F., Mater. Trans. JIM 48 (2007) 1739.
[11] L.C.R. Aliaga, M.F. de Oliveira, C. Bolfarini, W.J. Botta, C.S. Kiminami, J. Alloys Compd. 354 (2008) 1932–1935.
[12] L.C.R. Aliaga, C.S. Kiminami, M.F. de Oliveira, C. Bolfarini, W.J. Botta F., J. Non-Cryst. Solids 354 (2008) 1932.
[13] M. Matsuura, M. Sakurai, K. Suzuki, A.P. Tsai, A. Inoue, Mater. Sci. Eng. A226–228 (1997) 511.
[14] M. Matsuura, M. Sakurai, S.H. Kim, A.P. Tsai, A. Inoue, K. Suzuki, Mater. Sci. Eng. A217–218 (1996) 397.
[15] H.Y. Hsieh, T. Egami, Y. He, S.J. Poon, G.J. Shiflet, J. Non-Cryst. Solids 135 (1991) 248.
[16] H.Y. Hsieh, B.H. Toby, T. Egami, Y. He, J. Mater. Res. 5 (1990) 2807.
[17] A.N. Mansour, G. Cibin, A. Marcelli, T. Sevastyanova, G. Yalovega, A.V. Soldatov, J. Sync. Rad. 8 (2001) 809.
[18] A.N. Mansour, A. Marcelli, G. Cibin, G. Yalovega, T. Sevastyanova, A.V. Soldatov, Phys. Rev. B 65 (2002) 134207–134211.
[19] M. Matsubara, Y. Waseda, A. Inoue, H. Ohtera, T. Masumoto, Z. Naturforschteil 44A (1989) 814.
[20] A.N. Mansour, C.-P. Wong, R.A. Brizzolara, Phys. Rev. B 50 (1994) 12401.
[21] L. Zhang, K. Chen, X. Huang, Y. Wu, X. Bian, J. Phys.: Condens. Matter 13 (2001) 5947.
[22] R.D. Sá Lisboa, PhD Thesis, Federal University of São Carlos, Brazil, 2007.
[23] D.B. Miracle, Nat. Mater. 3 (2004).